ELSEVIER

Biophysical Chemistry 105 (2003) 621–637

Biophysical Chemistry

www.elsevier.com/locate/bpc

Hyperquenching and cold equilibration strategies for the study of liquid–liquid and protein folding transitions

C. Austen Angell*, Li-Min Wang

Department of Chemistry and Biochemistry, Arizona State University, Tempe, AZ 85287-1604, USA

Received 18 November 2002; received in revised form 10 February 2003; accepted 10 February 2003

Abstract

In this paper we consider the extension of the recent quantitative studies of hyperquenched glassformers to include (1) systems that exhibit first order liquid–liquid phase transitions, and (2) systems that contain molecules, which, during normal cooling, undergo internal structural changes above the glass temperature. The general aim of these studies is to trap-in a high enthalpy, high entropy, state of the system and then observe it evolving in time at low temperatures during a controlled annealing procedure. In this manner events that normally occur during change of temperature may be observed occurring during passage of time, at much lower temperatures. At such low temperatures the smearing effects of vibrations are greatly reduced. While the case of most interest in the second class is the refolding of thermally denatured protein molecules, any reconstructive molecular or chemical exchange process is a potential subject for investigation. Processes that occur in stages can be studied in greater detail, and any stage of interest can be frozen when desired, by drop of temperature, for more detailed spectroscopic examination. We review an electrospray method for hyperquenching liquids at approximately 10^5 K/s, and discuss some results of such experiments in order to illustrate a calorimetric approach to exploiting the hyperquenching-and- cold-equilibration strategy. To apply the idea to the study of proteins, the following protein solvent requirements must be met: (1) the solvents must not crystallize ice on cooling or heating, yet must not denature the proteins; (2) the solvents must support thermally denatured molecules without permitting aggregation. We describe two solvent systems, the first of which meets the first requirement, but the second only partially. The second solvent system apparently meets both. Preliminary results, only at the proof of concept stage, are reported for cold refolding of lysozyme, which, it seems, can be trapped in our solvent in the unfolded but refoldable state, with only moderate (approx. 120 K/s) quenching rates.

Keywords: Hyperquench; Protein folding; Liquid-liquid transition; Cold refolding; Renaturation; Fictive temperature; Energy landscape; Aggregation; Crystallization; Glass transition

*Corresponding author. Tel.: +1-480-965-7217; fax: +1-480-965-7972.
E-mail address: caa@asu.edu (C.A. Angell).

0301-4622/03/$ - see front matter © 2003 Elsevier Science B.V. All rights reserved.
doi:10.1016/S0301-4622(03)00093-0

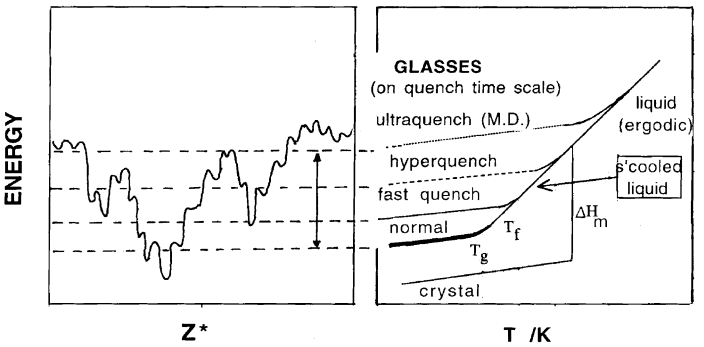

Fig. 1. Depiction of the relation between the landscape energy of the basin in which the system is trapped during quenching, and the rate of the quench. The familiar 2-D cartoon of the 'landscape' shown here is misleading in important ways, but this is not dealt with in the present paper.

1. Introduction

In the study of liquid state phenomenology, much insight has been gained over recent decades by the deliberate investigation of systems that can be studied at temperatures that are low, relative to the forces that control the motion of the particles. Such systems are typically viscous, and at lower temperatures they lose all diffusive motion and become glasses [1]. Following the surge of interest in the 'glassy dynamics' problem stimulated by the arrival of mode coupling theory (MCT), for the viscous slow-down process [2–5] there has developed a renewed interest in the 'energy landscape', whose interbasin barriers in configuration space [6–12] provide the escape from the critical rigidification predicted by MCT. Important progress in the statistical mechanical description of the liquid state is currently being made by exploiting the barriers to separate configurational from vibrational aspects of the liquid thermodynamics and to provide the basis for a 'landscape equation of state' [13–16].

The separability of degrees of freedom is manifested most directly in the phenomenon known as the glass transition [17]. The glass transition is characterized by the 'glass temperature' T_g defined as in Ref. [17], but it extends over a temperature range of 3–10% of T_g, depending on kinetic factors. Through the glass transition, the configurational contribution to the liquid heat capacity drops out, and the heat capacity therefore sharply decreases. It drops out because its exploration time scale exceeds that of the experiment that measures the heat capacity. Then the system is trapped in one of the vast number of minima on the landscape and thereafter acts like a crystalline (single structure) system, in which only vibrational modes can be excited. Seminal work in this area was performed by Walter Kauzmann, and his 1948 paper on the subject of entropy crises in supercooling liquids [18] remains one of the most influential in the field.

1.1. The fictive temperature

The energy of the basin in which the system becomes trapped during continuous cooling is higher, the higher the cooling rate. The potential energy of the trapped state can be depicted for different cooling rates, as in Fig. 1. The trapped state can be characterized by its 'fictive' temperature, T_f, [19] as indicated on the diagram. T_f relates to potential energy while the 'real' temperature relates to kinetic energy. When the two temperatures are the same, the system is a liquid. Otherwise it is a glass.

In principle, the fictive temperature can be measured by observations made during cooling but, when the cooling rate becomes high, such observations become difficult or impossible. Then the fictive temperature can be assessed by calorimetric measurements performed on the quenched glass during its reheating, as described in detail in

recent papers [20,21] which relate back to early studies by Moynihan and co-workers [22].

Some recent studies of this type for a molecular system will be reported below in order to illustrate (1) how mobile the glasses of high fictive temperature may be, at temperatures far below the normal T_g, and (2) how some features of the potential energy surface, that are not obvious from ergodic measurements, can be revealed. Then we turn to liquids of abnormal types that, despite intense investigations, seem not to have been studied this way before. These are liquids that exhibit first order transitions, either in bulk or at the single molecule level as in protein solutions. In these we have the possibility of examining processes like folding under conditions very different from those normally studied, namely, under cold equilibration conditions where the usual entropy/enthalpy compensation does not hold.

1.2. Quenching in first order liquid–liquid transitions, and high energy states of molecules

The fictive temperatures we want to obtain in the present study are those which lie above the temperatures at which the first order processes, referred to above, occur. The type of system that we wish to study can be depicted in Fig. 2, in which the sudden change of enthalpy at T_1 is due to the liquid–liquid transition. The aim is to trap the system in the glassy state before the low temperature phase can form (by nucleation and growth). The mechanism of the phase transition can then be studied during reheating. This trapping has already been achieved, first in simulation studies by Grabow [23] for the case of liquid silicon, and second, in the laboratory for the case of Y_2O_3–Al_2O_3 glasses, by McMillan and coworkers [24,25]. In neither case has it yet been fully exploited for the kinetic information on the process it should be able to yield.

In the molecular case of folding proteins, the sudden enthalpy change of Fig. 2 is replaced by a sharp but continuous change as the denatured protein molecules fold into their low energy (biologically active) forms. The distinction between the two arises because, whereas the bulk phase change between two isotropic liquids occurs at a

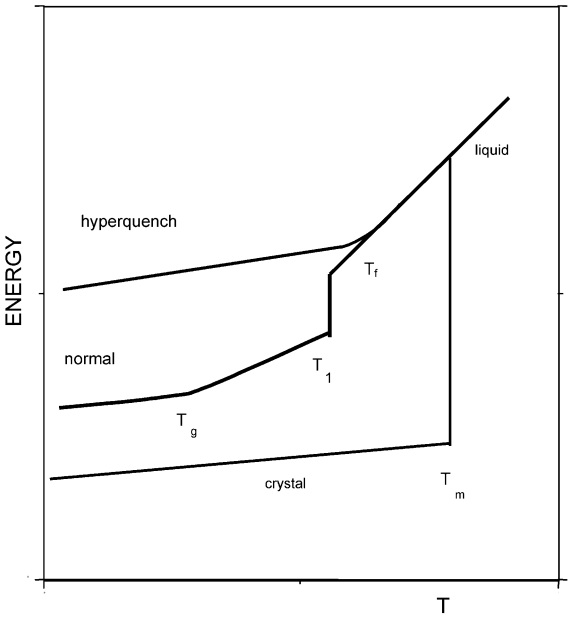

Fig. 2. Depiction of the manner in which hyperquenching of a system in which a first order liquid–liquid transition occurs not too far above T_g, can result in the suppression of the first order transition and the vitrification of the high temperature phase. Note that, on upscanning the system at the standard rate, a glass transition for the high temperature phase will only be manifested if the phase change has a significant activation energy, greater than that for the relaxation out of the basins of attraction that the system has been trapped in during the hyperquench. Otherwise it will relax to the low temperature liquid phase before the time scale for the standard glass transition is reached.

precise temperature for a given pressure, the mesoscopic process does not. The process that occurs in dissolved and uncorrelated subsystems, (assuming no aggregation of the subsystems is allowed—see Experimental section) takes place at different points within an otherwise homogeneous medium, and is subject to small system effects. Thus, it is smeared out over a range of temperatures, even when the molecular change itself (i.e. the sub-system process) is precisely two-state in nature. However, the main idea, which is to suppress the process of interest for leisurely study at lower temperatures, applies equally well to each case.

The observations to be made during re-heating of a system with fictive temperature T_f in Fig. 2,

($T_f > T_1$), will depend on the kinetics of the first order, or quasi-first order, process. During the reheating of simple glassforming systems, the processes that normally occur just below the fictive temperature in the equilibrated liquid, are the first to occur during the re-heating scan (i.e. they occur at the lowest temperatures). However, this is because they are intrinsically the fastest processes that were frozen in. The generation of a new phase, or the folding of a complex molecule into a specific 3-D form, are each likely to be intrinsically slow relative to the motions within the medium (within the high temperature liquid phase, in the first case). What then will happen during re-heating of a hyperquenched state of the liquid in which the liquid has been trapped at a temperature between T_1 and T_m as in Fig. 2?

What will happen will depend on whether the energy barrier responsible for the slowness of the process in the liquid state decreases with decreasing fictive temperature or not. Only a brief account can be given here, but this is the stuff of Kauzmann's seminal paper on glassformers. There he argued [18] that the size of the homogeneous crystal nucleus is decreasing as temperature decreases and so somewhere between the normal glass temperature and what is now called the Kauzmann temperature, the nucleation barrier would vanish. Indeed, this seems to be the case with many hyperquenched simple liquid systems. Crystallization during reheating commences before T_g is reached, and then the glass transition is never seen. This is certainly the case with the majority of metallic glasses, glasses that can only be formed by hyperquenching [26,27]. It is also probably (but controversially [28–30]) the case with amorphous water.

In the case of weak transitions that do not cause the system to leave the amorphous state, the trapped heat of the first order transition would be released well below the glass transition, like the frozen-in enthalpy of the normal hyperquenched glassformer [20,21], but presumably more suddenly. This sort of behavior is sketched in panel (b) of Fig. 3, which shows a variety of possible outcomes of such experiments.

On the other hand, if the barrier remains high, or the process cannot occur because it requires substantial reorganization of the surrounding medium, then the suppressed first order transition might only be manifested above the normal glass transition temperature, as in panel (c) of Fig. 3. This seems to be the behavior of the first order polyamorphic transition in Y_2O_3–Al_2O_3 glasses [24,25]. Wilding and coworkers found they could quench in a clear glassy state, which would release heat suddenly, during heating above the glass transition. After the initial exotherm, the material still showed no Bragg peaks so the heat release was assigned to the heat of the quenched-in liquid–liquid transition (see Discussion). The presence or absence of a barrier to the first order process, or related mesoscopic process, would be

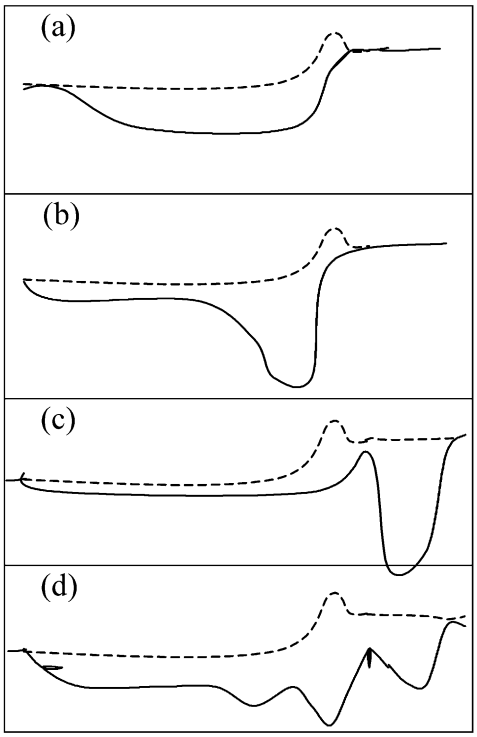

Fig. 3. Depiction of the possible ways (b, c and d) in which systems with complexity above the normal glass temperature (polyamorphic transitions, molecular folding, etc) might relieve quenched-in instabilities during upscans. Comparison is made with the case of simple glassformers, depicted in part (a). In each panel comparison is made with the 'standard' scan shown as a dashed line.

the first point that our proposed study should help establish.

If the phase transition, or the folding process, were also to occur in different stages, characterized by increasing activation energies, then it may well be observed to occur in successive exotherms during re-heating from the quenched-in state. This scenario, which is made possible by the conditions of reduced vibrational smearing characterizing the low temperature anneal, or scan, is illustrated in Fig. 3d. The possibility of revealing such stages in the folding of proteins thought to be two-state folders, is a second major reason for undertaking this study.

There are further possibilities to be mentioned by way of suggesting the potential richness of hyperquenched complex system phenomenology. Suppose a molecular reconstruction process that occurs in a rapidly relaxing medium under ergodic conditions is slow, but not first order. Then during quenching its state of equilibrium will become trapped at a fictive temperature (a second fictive temperature) that is much higher than the fictive temperature of the matrix. This second fictive temperature will also be dependent on the quench rate. An example is the chain structure of sulfur that forms above the well-known $\mu-\lambda$ transition at 160 °C. This structure may be easily frozen-in to give the 'plastic sulfur' phase, which is a rubber. With respect to the chain structure itself, the fictive temperature of rubbery sulfur is well above 160 °C. On the other hand, the standard fictive temperature for the glass of this phase, determined by the Moynihan equal area construction at T_g [22] is approximately -31 °C. Thus the system is characterized by two fictive temperatures, one for the medium range order and one for the short range order. This is like the case of arrested composition fluctuations described recently [31], in which the need for a second fictive temperature was in focus. The isocompositional cases have been treated theoretically by Stillinger and Weber for sulfur [32], and by Kumar and Douglas [33] for 'living polymers'.

Additional cases of a different type are illustrated by the sugars, fructose and galactose, in which the slow process (due to an internal molecular rearrangement) is manifested as a second T_g-like process within the fluid phase domain. This second glass-like transition has caused much confusion [34]. In these cases, normal DSC instrument quenching of the samples produces effects that, for the slow process of interest, are only manifested far above the first (normal, low temperature) glass transition [34].

Thus there are many different possible outcomes for such experiments. This makes their investigation, for processes such as the refolding of proteins (and link-up of hairpins), the rearrangement of complex molecules, and the first order polyamorphic transition in certain liquids (e.g. Refs. [24,25]), a matter of some interest.

In this introduction we have made no attempt to review the huge literature on the folding of proteins, since we will not make any interpretations of our observations. Rather, we just note the major contributions of Walter Kauzmann and his coworkers [35–38] to this fascinating and important problem, and offer the possibility of additional experimental information that may be found useful for such interpretations.

2. Experimental section

This section has two components. First, we give a brief account of a method, described in more detail elsewhere [39], for producing glassy droplets from liquids that have been vitrified at cooling rates of approximately 10^5 K/s. Secondly, we describe the sample preparation methods that have been developed as a necessary preliminary to a successful application of quench-and-scan approach to protein folding studies. For the protein that we have studied, lysozyme, dissolved in the solvents we have developed, it has proven unnecessary to use hyperquenching rates to suppress the refolding. Simple pan-quenching in liquid nitrogen suffices. However, it is likely that hyperquenching will be needed to study the so-called fast folders that we hope to investigate in follow-up studies.

2.1. Hyperquenching method

Concerning hyperquenching, we stress at the outset that much work on the problem of maximizing quench rates has been done in the past

three decades (see [26], commentary in Ref. [20], and other literature cited there). The great majority of the studies have been directed at preventing crystallization rather than for the present purpose of preserving high temperature liquid structures of naturally glassforming systems, for subsequent study, i.e. for fundamental liquid state studies.

Among the different hyperquenching techniques, the electro-spray method for producing fine particles and filaments is particularly suitable for in situ preparation of samples for DSC study We will present some recent results utilizing this method. The apparatus [39] consists of a fine syringe needle located in the dry box housing of the DSC head directly above a DSC pan in close contact with an aluminum pedestal that is mounted in a small liquid nitrogen bath. Between the needle and the pedestal is established a 10 000 V potential difference. As the test liquid flows out of the syringe at a steady controlled rate, the electronic charge acquired by the surface breaks the stream up into tiny micron-sized droplets. These impact on the cold DSC pan, and are collected in spaced bursts, such that a cold surface is always encountered. Cooling rates in of 10^5 K/s are demonstrated in Ref. [39] (see also Ref. [28]), and rates in excess of 10^6 K/s have been obtained for other systems, e.g. for liquid silicon [40,41].

Each liquid sprays optimally at different voltage and flow rate conditions—which must be determined empirically. Below we will show results obtained for the somewhat water-like, −OH containing, molecular liquid propylene glycol, which has very satisfactory electrospraying characteristics.

To utilize the quenched or hyperquenched samples for study of the quenched-in state and its relaxation to the normal state, we compare the thermal behavior of the hyperquenched sample with a 'standard scan' of the same sample. The standard scan is one in which the heat flow is measured during an upscan at the standard scan rate of 20 K/min after preparing the sample initially by cooling it through the glass transformation range at 20 K/min. For comparison, the quenched sample is upscanned at the standard rate, and the two scans are superposed using the data at temperatures (1) below that of the relaxation onset of the quenched sample, and (2) above the glass transformation range, 1.1 T_g, where all traces of the sample history disappear.

2.2. Solvents for protein refolding studies

For study of the low temperature protein refolding energetics using standard differential scanning calorimetry techniques, two problems need to be overcome. The first is the tendency of unfolded protein molecules to aggregate and thereby become incapable of refolding. The second is the interference with the thermal signals of interest (i.e. those due to refolding) by signals due to other processes. The main problem in this respect is the exothermic signal due to ice crystallizing from the vitrified sample, and the endothermic signal from ice remelting as the temperature rises above 0 °C.

Thus we need to develop solvents that discourage the segregation phenomenon common to concentrated protein solutions and which, at the same time, suppress ice crystallization during quenching (and, more difficult, ice crystallization during rewarming). Since the presence of considerable water content is usually considered necessary for the stabilization of the folded protein structure, and in particular for refolding after denaturation to be possible, such solvents would seem unlikely to exist. However, it appears from data presented below that the second problem (avoiding ice) can be solved by adding sufficient concentration of the dissacharide sucrose (and no doubt others as well). It further appears that the first problem (aggregation) can be solved by including the room temperature ionic liquid, ethylammonium nitrate, in the solution. The usefulness of this ionic substance in supporting the refolding of proteins has earlier been described by Flowers and co-workers [42,43].

Although the latter solutions are obviously the more desirable, we will include results for the former by way of showing the development of the method.

2.2.1. Preparation of aqueous sucrose solutions

Lyophilized lysozyme from hen egg-white (Sigma, batch no. L-6876) was dissolved in water to give a clear solution, and then weighed quantities of sucrose were dissolved to provide a viscous

solution of known wt.% sucrose. Freshly prepared solutions gave strong denaturation endotherms, even up to 78 wt.% sucrose. However, such solutions, when held overnight at room temperature, lost signal strength due to some undetermined processes (probably aggregation). For the sucrose-only solutions described below, freshly prepared samples had to be used in most tests in order to establish the proper background data.

Solutions up to 65 wt.% sucrose showed small residual ice crystallization peaks during reheating. The lysozyme was found to refold in good proportion after denaturation (at temperatures as high as 100 °C) even with sucrose concentrations high enough (78 wt.%) to completely suppress ice crystallization. The solution viscosity alone discourages aggregation. The glass transition temperature is low enough to support low temperature studies, but is higher than desirable, approximately −40 °C, depending slightly on the state of the protein.

In the sucrose solutions, a certain amount of protein is lost after the initial denaturation, presumably to aggregation, though the residual re-foldable fraction seemed to be fairly stable. This stabilization phenomenon might have been worth further investigation, but the question is rendered moot by our subsequent success in largely eliminating aggregation by the inclusion of ethylammonium nitrate in the solution.

2.2.2. Preparation of ethylammonium nitrate, and ethylammonium nitrate + sucrose, aqueous solutions

A very satisfactory solution medium for protein studies is achieved by combining ethylammonium nitrate (a room temperature ionic liquid) with sucrose (or other sugars). An initial solution of 20 mol% ethylammoniuim nitrate in water was used as a base for addition of sucrose, up to 34 wt.%, and lysozyme (approx. 21 wt.%). The final mass distribution in a solution designated '30 wt.% sucrose' (see figures below) is as follows: water 20 wt.%, ethylammonium nitrate 29 wt.%, sucrose 30 wt.%, lysozyme 21 wt.%.

A study of the phase diagram and glass formation range will be published elsewhere. We note here that solutions above 30 mol% are glassforming without any further components being needed. However, they denature lysozyme.

Solutions of 20 mol% ethylammonium nitrate and 80 mol% water, to which 27–34 wt.% sucrose is added, not only totally avoid ice crystallization during cooling and reheating, but their solutions of lysozyme yield almost constant denaturation signals on multiple heating/cooling cycles. These solutions have very low glass transition temperatures, close to −100 °C, so that, after initial quenching, they offer a wide temperature range in which thermal events related to the refolding can be studied at leisure. In the absence of protein content, the solutions show completely uneventful (flat) scans, from above the glass transition to well above 100 °C where decomposition of the sugar will eventually take place.

Only pan-in-liquid nitrogen (LN_2) quenches, and DSC instrumental quenches, have so far been carried out on the protein solutions. For lysozyme, these quenches seem to be sufficient to suppress refolding completely or partly (respectively). The possibility of hyperquenching solutions of very fast-folding proteins will be investigated in future work.

3. Results

3.1. Hyperquenched molecular liquids

In Fig. 4 we compare standard scan and quenched sample scans for two cases quenched at two different rates. The upper pair of curves is for a sample that was initially quenched by dropping it, in a hermetically sealed aluminum pan, into a bath of liquid nitrogen, before cold transfer to the DSC head for upscan. The lower pair is for a sample that was electrosprayed into an open DSC pan as described in the previous section, before cold transfer to the DSC head. The difference between the energies trapped in the two cases is immediately seen in the much larger area lying between the standard scan and the quenched scan in the case of the electosprayed sample. The effect of changing the cooling rate, under instrument control, between 5 and 40 K/s can be seen in Fig. 5. At these much lower cooling rates the difference between standard and non-standard scans is seen

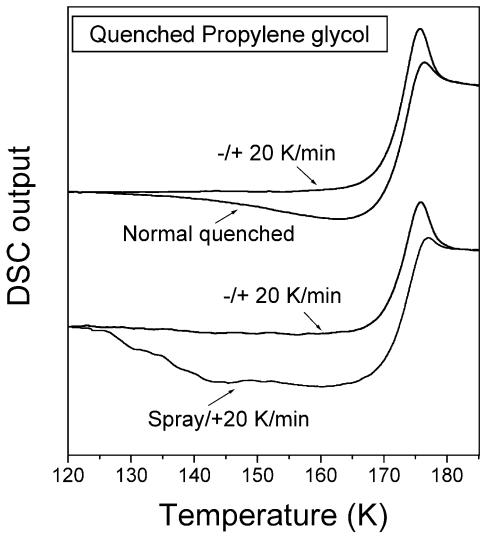

Fig. 4. Comparison of the upscan (at standard scan rate) of quenched samples, with standard samples for the case of propylene glycol. The upper pair is for a sample, in sealed pan, dropped into liquid nitrogen, while the lower pair is for electrosprayed sample in open pan. The much larger frozen-in enthalpy of the lower case is seen in the much larger area between the two scans for this case.

mainly in the immediate vicinity of the glass transition, whereas in the case of higher quench rates the difference is manifested at increasingly lower temperatures. Fig. 5 is used to obtain the data needed to estimate the quench rate from the data of Fig. 2. The way in which the areas lying between the standard scan and scans at other non-standard cooling rates can be used (see Fig. 4 inset) to obtain the fictive temperatures has been described adequately elsewhere [20,21,44] and need not be repeated in detail here.

The fictive temperatures obtained are plotted in a reduced form in Fig. 6. The slope (and intercept) of this plot both yield the liquid '*m* fragility' [45,46] or steepness index [47], with a precision which is not exceeded by that of any other technique, as recently documented in detail [44]. The value of *m* reported on the basis of dielectric relaxation measurements in Ref. [48] is 54.

The data of Fig. 6, guided by the form of the dielectric relaxation temperature dependence [48] which is shown as a dashed line in Fig. 6, can now be used to estimate the hyperquenching rate. This rate is obtained from the intersection of the scaled quench rate with the vertical line representing the fictive temperature obtained for the hyper-

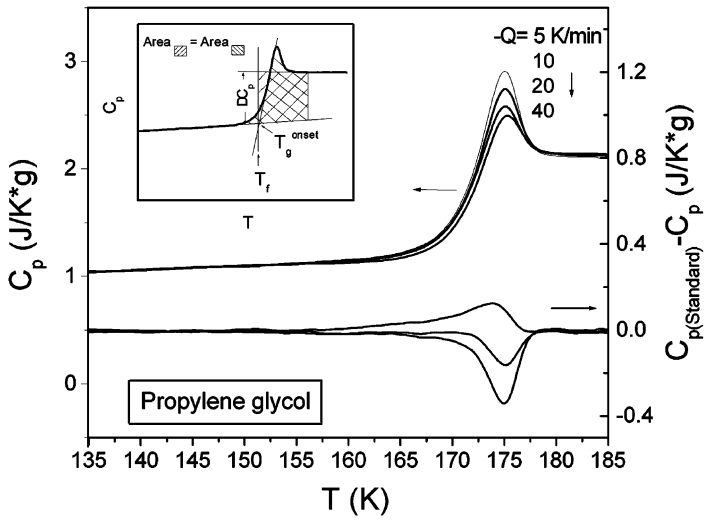

Fig. 5. Upscans of samples cooled under instrument control at different rates, including standard rate of 20 K/min, (left hand ordinate) and the differences between standard and non-standard scans (right hand ordinate, lower curves). The insert shows how the fictive temperature T_f, used in the Fig. 6 plot, is obtained in each case.

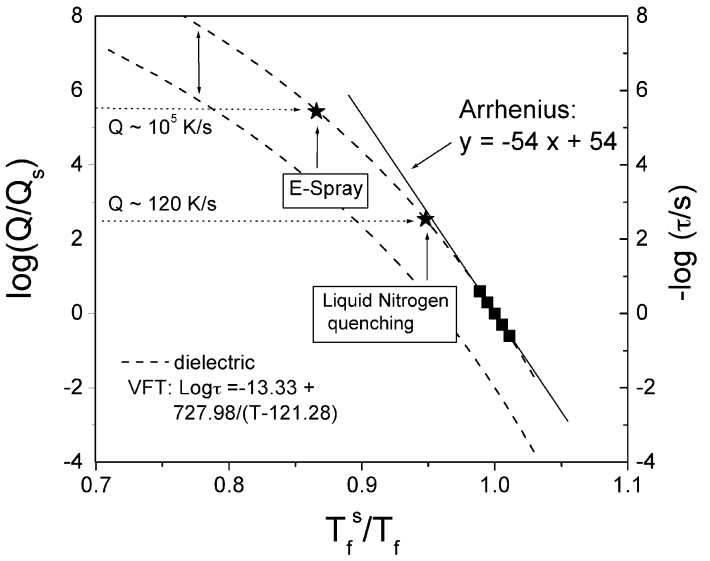

Fig. 6. Arrhenius plot of reduced fictive temperature vs. reduced quenched rate, using standard values as scaling parameters. The full curve is the plot of dielectric relaxation times (from Ref. [48]), which are matched to the fictive temperature data near T_f^s, and used to guide the extrapolation to the reduced fictive temperature of the hyperquenched sample. The value of the reduced quenching rate at this latter reduced fictive temperature yields a quench rate for the hyperquenched sample of $10^{5.5}$ K/s, while for LN_2 Pan quenching, -Q is 120 K/s. The parameters of the Vogel–Fulcher–Tammann (VFT) equation best fitting the relaxation time data [48] are given in the legend.

quenched sample, by the same area integration method. The fictive temperature was found to be 194 K, or 1.15 T_g. According to Fig. 5, this indicates a quenching rate of 10^5 K/s after taking account of the quench rate of the standard scan. This is close to the value estimated for the aerosol droplet method of Mayer [49,50], applied to the case of di-ols by Mayer and coworkers [51]. Indeed, the temperature at which their (incomplete) upscan of the hyperquenched glass departs from the plots for ordinary scans ([51], Fig. 4), is the same as ours to within the uncertainty of determination. In considering the reliability of our Fig. 6 estimate of the quenching rate obtained in the electrosprayed sample, it should be borne in mind that the dielectric relaxation times coincide with the ac heat capacity-based relaxation times for PG [52] in the range in which they overlap.

3.2. Protein solutions

Most data reported here are for sucrose solutions, because the more desirable ethylammonium

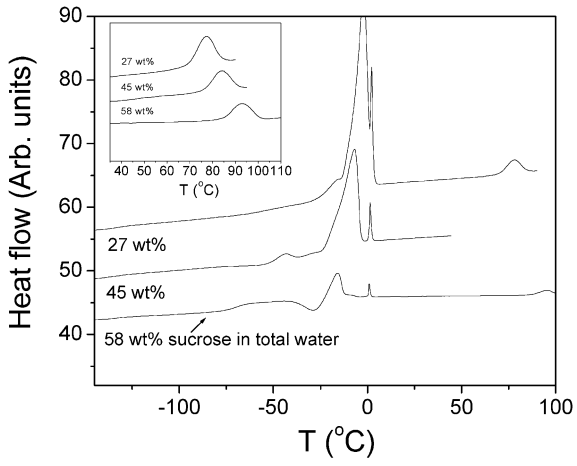

Fig. 7. Upscans of lysozyme-saturated sucrose solutions of different sucrose contents, after quenching at the maximum instrumental rate (5 K/s) from above the denaturation temperature. Denaturing upscans are shown in the insert. Only at 58 wt.% sucrose is the glass transition clearly seen followed by a weak crystallization of ice that almost immediately remelts. The second denaturation is seen near 90 °C.

nitrate-based solvent system was only developed after this paper was submitted for publication. More adequate evaluation of the preliminary promising results reported below for this type of system, will be given elsewhere.

Fig. 7 shows data for up-scans of lysozyme–sucrose-water solutions of different sugar contents scanned after (1) instrument quenching (at approx. 5 K/s, the maximum rate) to −140 °C and (2) after denaturation by heating to the end of the denaturation peak and immediately instrument quenching to −140 °C. The denaturation peak is seen (Fig. 7 insert) to be shifted from its normal temperature of 67 °C systematically to temperatures above 90 °C with increasing sugar content. We find it remarkable that the upscan made after the instrument quench from the fully denatured state, shows that a substantial fraction of the protein has refolded (either during the quench or during the slower upscan), as manifested by the second unfolding at the same temperature (Fig. 7 main part).

The large increase in the solution viscosity associated with the high sugar content makes the trapping of the protein in the unfolded state much easier to achieve. For such conditions, hyperquenching becomes unnecessary and the liquid nitrogen quench we have used in these preliminary studies seems to be adequate. In-pan quenching is certainly preferable as far as reproducibility of measurements is concerned. Hyperquenched samples will be investigated in subsequent studies to determine if any qualitative differences are to be found, and to study fast folders.

Fig. 8 shows a fresh sample of the high sugar content solution after its initial denaturation, following two different subsequent treatments. In the first, the denatured protein has been quenched from the denatured state at 102 °C by dropping the pan and contents into liquid nitrogen. In the second, following the upscan shown as a solid curve, the sample was cooled from the unfolded state at 102−70 °C and held 5 min to allow every chance to refold, and then quenched into LN_2 as before. This procedure provides a control scan to separate out the effect of the ice crystallization. Any difference between this upscan and that of the sample quenched from above denaturation

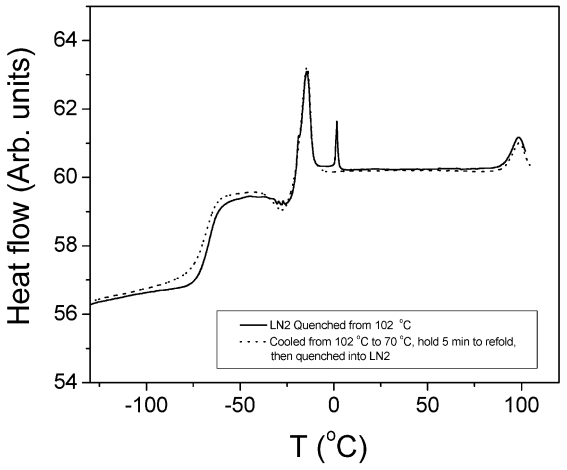

Fig. 8. Upscans of lysozyme-saturated sucrose + water solution (65% sucrose), after dropping pan into liquid nitrogen LN_2 to quench at 120 K/s. Solid curve is for the sample quenched from above denaturation at 90–100 °C, while dashed curve is for sample cooled to 70 °C after denaturation, held 5 min to renature, and then quenched into LN_2. Comparison shows exotherm due to renaturation near and above T_g.

temperature, can be attributed to the effect of low temperature renaturation. Differences are seen to be present in the vicinity of the glass transition, and will be discussed in the next section.

The presence of residual freezable water complicates interpretation of the rescans so additional solutions containing even higher sugar contents, namely 78 wt.% of the solution in which the protein was dissolved were prepared. From these no ice crystallized during upscans as seen in Fig. 9. Data on DSC-quenched samples are shown in the upper section of the plot, while scans for LN_2-quenched samples, following the protocol of Fig. 8, are shown in the lower section. One of the upper group was acquired before any denaturation and therefore shows the full unfolding endotherm. The loss of refoldable protein (presumably to aggregation) is indicated by the change in endotherm area before and after initial denaturation. After the intitial loss, the refoldable protein content appears almost stable, particularly for the lower two scans. As in Fig. 8 there appears to be an excess heat released in the upscan of the quenched unfolded sample in the vicinity of the glass tran-

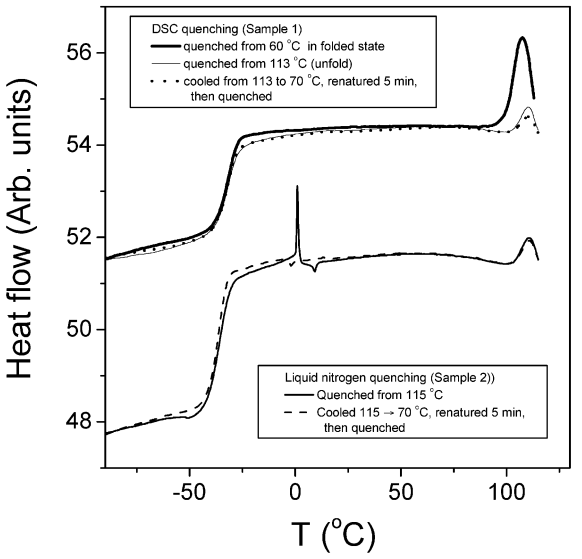

Fig. 9. High sucrose samples, 78 wt.%, in which no ice forms on reheating but refolding still occurs after denaturation and quenching. Upper curves are for samples quenched at the maximum instrument rate (5 K/s). Lower curves are for quenching 25 times faster by liquid N_2 quench. The latter show a distinct excess heat release near and above T_g for the sucrose–H_2O–protein matrix, for the case that was quenched from above denaturation relative to the same sample held at 70 °C to refold before quenching. The spike at 0 °C is attributed to trace water condensed on outside of pan during transfer to the DSC head after the LN_2 quench procedure. Upper curve includes initial denaturation, and comparison with subsequent scans demonstrates loss of some protein to aggregation after the initial denaturation.

sition and this is most marked in the LN_2-quenched samples.

Fig. 10 shows the more encouraging results for the lysozyme solutions in more fluid mixed ethylammonium nitrate+sucrose aqueous solutions described in the previous section. The complete recovery of the initial unfolding peak, after denaturation, quenching and reheating is a significant achievement. Samples have been cycled through the unfold/fold transition many times with only minor change of endotherm area. We note the complete absence of any signals due to ice crystallization or remelting. The sharp spike at 0 °C in panel (b) is, as before, attributed to traces of water condensed on the pan exterior during the transfer to the DSC head. Such contamination was evi-

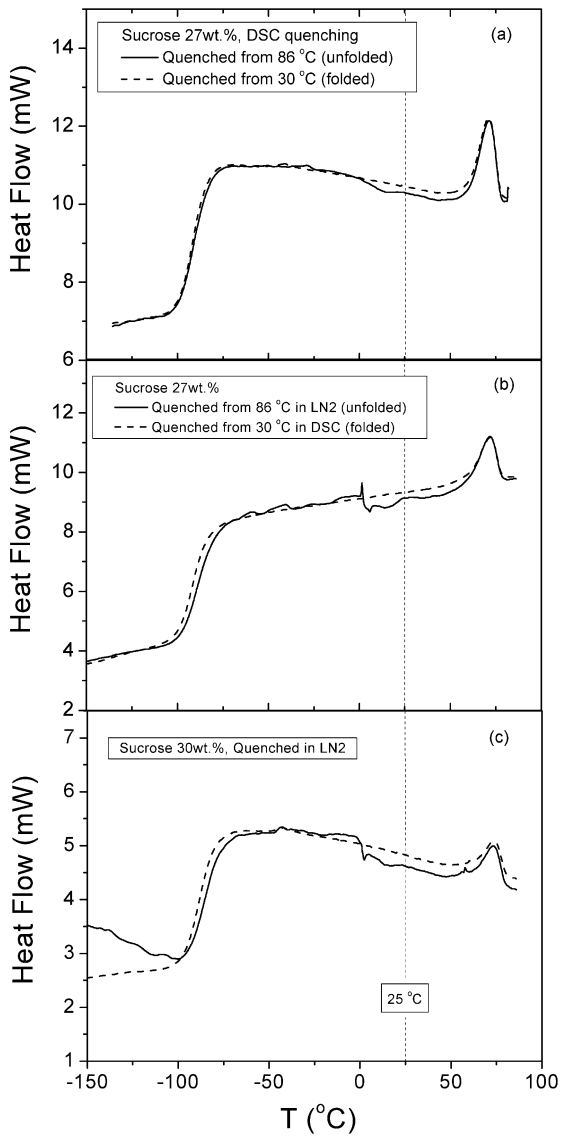

Fig. 10. Comparison of the upscans of solutions quenched from 30 °C (with lysozyme folded, dashed line) and quenched from 86 °C (lysozyme unfolded, solid line). The glass transition at −95 °C [panel (b), is slightly (∼5 K] raised by the presence of unfolded protein. The effect of interest is seen at $T>0$ °C, and is weak in the instrument-quenched sample panel (a) implying that much of the protein refolded during the quench. The larger effects seen in panel (b) and (c) for independently prepared solutions of different sugar content, are consistent with complete suppression of the folding during the faster (120 K/s) quench. Note the structure in the refolding exotherm, which seems to be common to each case. The sharp spike at 0 °C in panel (b) is attributed to trace moisture condensed on pan during dry-box transfer from LN2 quench bath to DSC head, and is not seen in panel (c).

dently successfully avoided in the case of the 30% sucrose solution seen in panel (c).

The differences between quenched native and quenched denatured scans are significant in all three cases but are more pronounced in the cases of liquid nitrogen quenching seen in panels (b) and (c). These are discussed below.

4. Discussion

In this section we will first discuss some of the information that can be obtained from the results of hyperquenching simple glassformers, and will then examine some findings from the more preliminary quenching studies of systems with additional complexity, namely the refolding protein systems.

4.1. Calorimetric quantification of initial trap characteristics

Using the data of Fig. 6, we can proceed to estimate the depth of the trap in which the sample was arrested during the hyperquench at 10^5 K/s and then to compare it with the energy of the trap minimum relative to that of the standard glass.

The energy of the trap minimum relative to that of the standard glass has already been obtained as part of the procedure for determining the fictive temperature. It is simply the integral of the difference between the two curves of Fig. 2 lower section. In the present case it amounts to 1.9 kJ/mole. Comparisons of this figure with relevant quantities (1) the enthalpy of fusion (2) the enthalpy of exciting the liquid from the glass temperature to the melting point and (3) the enthalpy of exciting the liquid from the Kauzmann temperature to the boiling point, have been made elsewhere [39]. All are found to be large relative to the 1.9 kJ/mol of trapped-in enthalpy. This was explained by the large dependence of the relaxation time on energy level in this regime near the glass temperature.

The trap depth on the other hand, is large relative to all of the above. It is found by making use of the fact that, for an upscan at 20 K/min, the system will start to release heat when the enthalpy relaxation time reaches 100 s. This is the relaxation time of the liquid at the glass transition temperature where relaxation commences in the standard scan, and it must also be the relaxation time for trap escape in the upscan of the hyperquenched sample.

Assigning an attempt frequency of 10^{13} Hz, the energy of the barrier opposing the relaxation can then be obtained from the Boltzmann probability, per attempt, of escaping from the trap at the temperature T_{esc}, viz.,

$$p_{(\text{escape})} = \exp\text{-}(E_{\text{trap}}/RT), \tag{3}$$

from which

$$100 = 10^{-14}\ \exp(E_{\text{trap}}/RT),$$

and

$$E_{\text{trap}} = 2.303\ RT_{\text{esc}}\ \log(10^{16}) = 37\ RT_{\text{esc}} \tag{4}$$

The trap depth for the present case of hyperquenching, in which Fig. 4 shows escape commencing at 125 K, is therefore 39.9 kJ/mole which is, as pointed out in Ref. [39], considerably in excess of the height of the energy landscape. The latter was estimated to be approximately 20 kJ/mol for a constant volume system with volume fixed at the value at the glass temperature.

The same value for the trap depth is obtained by the construction suggested by Dyre [53] to avoid the confusion arising from the fact that, when the temperature changes, the structure changes.

The Dyre construction is, in turn, the same one suggested by conductivity measurements made on ionic glassformers in which a subset of mobile ions move much faster than the average [54]. In these, the conductivity can be measured below T_g where the structure has become fixed. Then the conductivity conforms to the Arrhenius law with pre-exponent close to the physically meaningful inverse attempt frequency for the conduction process [54], the low frequency (far IR) optical phonon frequency. To obtain the physically meaningful activation energy at the temperature where the system froze during the hyperquench (obtained as in Fig. 6), one draws the straight line between the relaxation time at the fictive temperature and

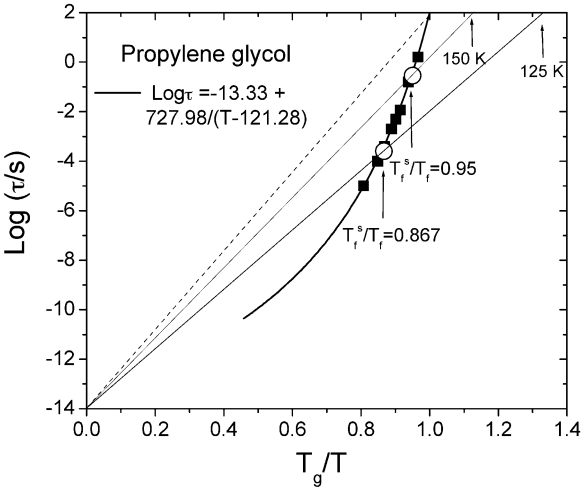

Fig. 11. Assessment of the activation energy for relaxation of quenched glasses out of their trap sites, using the scaled fictive temperature, T_f^s/T_f. Values for the hyperquenched, and pan-quenched samples of this study, are shown by open circles. Extrapolation of the straight line construction to log $\tau = 2$, predicts the temperature at which a glass of this fictive temperature will start to relax during warm-up at the standard DSC heating rate of 20 K/min, which are indicated by arrows. The relaxation time data (solid squares in the figure) are from Ref. [48]. Vogel–Fulcher–Tammann equation parameters for the dielectric relaxation time are given in the legend.

the pre-exponent for the process. The slope of this line yields the activation energy according to the usual relation $E_A = \text{slope} \times R\ln 10$.

The consistency of this construction with the earlier assessment using Eq. (4), is seen from Fig. 11, in which the straight line from the pre-exponential time (an inverse vibration frequency) through the fictive temperature of the hyperquenched glass, passes directly through the (Fig. 4) escape temperature of 125 K.

4.2. Universal activation energy for glassformers at T_g

For the less rapidly quenched glass the trap depth is clearly greater, see Fig. 11, and it reaches its maximum value for un-annealed glasses formed at normal cooling rates, when the fictive temperature becomes T_g. The activation energy at T_g, which is now seen to be universal for glasses, at the value $E_A = 16 \times 2.303RT_g$, reaches 53.9 kJ/mol for propylene glycol. This is comparable with the quasi-lattice energy of the substance [39]. In Ref. [39], this value has been compared with the activation energy for diffusion in crystalline systems in which diffusion is a single molecule process. If the magnitude of the activation energy were to be taken literally it would imply a need to modify considerably the common depiction of the energy landscape given in Fig. 1. Near T_g, any 2-D cartoon of the potential energy surface would look much more like the profile of an alarmed hedgehog than a 'landscape'. The meaning of 'activation energy', when applied to glass-forming systems, may need re-interpretation so as to avoid the implication that it requires much more energy to move a molecule from one site to another (and in so doing move the system from one metabasin to another at the same landscape level) than it does, per molecule, to move the system from the Kauzmann temperature to the 'top of the landscape'.

The activation energy for commencement of any other process occurring within the glassy state and requiring gross rearrangement of the glassy structure, should likewise involve a comparable activation energy. On the other hand, decoupled processes like fast ion motion, and gas diffusion, and small molecule penetration, may involve much smaller energy barrier crossings. Indeed, such low barrier modes of motion are of critical importance in biology where they permit the loss of water and consequent anhydrobiotic protection of seeds and organisms.

4.3. Refolding energetics

We referred earlier to the findings of McMillan and colleagues [24,25] for the liquid–liquid transition in Y_2O_3–Al_2O_3 liquid, studied by first quenching the liquid. They showed [25] that the heat of the liquid–liquid transition, as studied by upscan DSC, or dissolution studies, of the quenched glass, was small relative to the heat of crystallization. It amounted to some 10%, quite similar to the value found for the liquid–liquid transition in silicon [23]. The value was seen to depend on composition, just as the value in the single component silicon must depend on pressure,

and vanish at a liquid–liquid critical point. No further information on these transitions has been acquired in the present study. Rather, we have sought to acquire comparable information on the mesoscopic version of this transition

Relative to the findings for the bulk transitions, and to the insights on energy landscapes provided by the data of Fig. 4 and analyzed above, the information made available on the more complex matter of folding mechanisms by the preliminary quenching studies seen in Figs. 7–9 for sucrose solutions, is disappointing. This is partly due to the difficulties of separating the effects of interest from the effects of crystallization of residual water. Partly, also, it is due to the problems of sample preparation and problems of signal-to-noise ratio with the modest quench rates we have been able to apply to date given the loss of refoldable protein. There seem to be distinct differences between the behavior observed when the protein has never been unfolded or, alternatively, has been given every chance to refold, and the behavior when it has been quenched from the unfolded state, but the differences are not significant enough to warrant interpretation.

Disappointment in the results of Figs. 7–9, however, is alleviated by the data in Fig. 10 for the less viscous solutions containing ethylammonium nitrate. In these, aggregation did not occur and refolding could be obtained repeatedly. Here there is room for some optimism. Not only do we observe the presence of effects that scale with the quench rate, but we see effects that are reproducible between samples of different preparation and different solvent compositions (27 vs. 30 wt.% sucrose). The area under the cold refolding curve is close to the area under the denaturation curve(s) in the case of the liquid nitrogen quenched samples, and there is structure in the refolding curves which is reproduced in the two independent samples. The refolding seems to start abruptly near 0 °C and be followed by a slow-down near 5 °C, an acceleration near 15 °C, followed by a further slowdown near 30 °C and acceleration beyond. The coincidence of the sudden start with 0 °C suggests an artifact associated with external ice contamination from the quench bath, though the absence of a melting peak in the panel (c) case means the source of the effect will need further investigation.

We regard these results as strictly preliminary, but must note some semblance to the multistage phenomenon envisaged in the construction of panel (d) of Fig. 3. In the lysozyme case, however, no event is detected below T_g, nor indeed until far above T_g where the matrix is quite fluid. This is consistent with what is already known from structural studies of lysozyme refolding initiated by cold dilution from a chemically denatured state [55]. In those studies also no events are observed below 0 °C. Hopefully, our studies might provide an energy profile to accompany the detailed structural profile provided by Ref. [55] and its forerunners, since our denaturation temperature and also denaturation enthalpy are imperceptably different from those of the process occurring in standard biological media [42,56,57]. Comparisons with the cold equilibration of other quenched-in n-state processes will be shown in a subsequent paper.

In addition to clarifying the origin of the apparent abrupt start, we that lysozyme is a two-state folder [58,59], and the more current understanding [54 and W.A. Eaton, personal communication] that it is a three-state folder. This issue will be studied by anneal-and-scan methods like those of Yue and co-workers for glasses [60,61], multistep annealing studies, and anneal-and-scan studies, to be conducted in future work on the quenched samples. The dependence of the Fig. 10 scans on quench rate and solvent composition will also need careful evaluation.

It is perhaps not surprising that, at the 20 K/min upscans of this work, there are no signs of lysozyme refolding at temperatures lower than 0 °C. Processes with time scales longer than 100 s are not detected by these scans. When temperature is reduced, the large entropy decrease that accompanies folding will not be effective in restraining the large energy drive to fold, but the activation energy for the process will slow down all but the fastest elements very rapidly. The situation may be rather different in the case of ‘fast folders’. Attempts to relate our observations to the evidence for two-state and multistate folding scenarios that are the subject of such a large literature, would be quite premature. Eventually it might be hoped to

add some detail to, or confirmation of, the folding funnel [62–64], or critical nucleus [65,66], scenarios and their variations, many of which are reviewed in Refs. [67] and [68].

In future studies we will characterize the solvent relaxation times, optimize their compositions, and vary the protein concentration—and of course will look at other proteins in the same solution. Anneal-and-scan studies will extend the time scale over which refolding can be studied. If the promise of these early studies is borne out, further physical properties including the usual spectroscopic characterizations will be attempted.

5. Concluding remarks

The essence of this approach to liquid and protein studies is to replace temperature, as the key variable, with time, so that system evolution can be studied at low temperatures. The most desirable case for study would be one in which the entire process of equilibration could be carried out at a single temperature. For simple glassformers, this is not a practical possibility because at temperatures where the initial stages of the relaxation are slow enough to be followed, the system is close to its Kauzmann temperature. Therefore, it could never be observed to reach equilibrium. However, for a case where there is a quenched-in first order transition the exploration of the kinetics of the phase transition during recovery might be determined in this manner. The best possibility would be the measurement of an extensive property like volume over a series of anneals to a quasi-equilibrium, or non-evolving state—followed by an increase of temperature and a further anneal to quasi-equilibrium. In this way the kinetics of exploration of the energy landscape at different levels on the landscape could be determined. This sort of study was recently performed for a sample of high density amorphous water, observed during annealing from the quenched-in high pressure state [69], though the observations were interpreted in a rather different manner.

Acknowledgments

This work was made possible by support of the NSF, Solid State Chemistry program, under Grant No. DMR-0082535. We are grateful to Wu Xu for synthesizing ethylammonium nitrate, to Barry Ninham for helpful suggestions concerning the repression of aggregation effects in denatured proteins, and to Pablo Debenedetti and Srikanth Sastry for helpful commentaries on the mansucript.

References

[1] C.A. Angell, Formation of glasses from liquids and biopolymers, Science 267 (1995) 1924–1935.
[2] U. Bengtzelius, W. Götze, A. Sjölander, Dynamics of supercooled liquids and the glass transition, J. Phys. C: Solid State Phys. 17 (1984) 5915–5934.
[3] W. Götze, in: J.P. Hansen, D. Levesque (Eds.), Liquids, freezing, and Glass Formation, Les Houches, 1989.
[4] T.R. Kirkpatrick, P.G. Wolynes, Connections between some kinetic and equilibrium theories of the glass transition, Phys. Rev. Part A 35 (1987) 3072–3080.
[5] T. R Kirkpatrick, D. Thirumalai, P.G. Wolynes, Scaling concepts for the dynamics of viscous liquids near an ideal glassy state, Phys. Rev. Part A 40 (1989) 1045–1054.
[6] M. Goldstein, Viscous liquids and the glass transition: A potential energy barrier picture, J. Chem. Phys. 51 (1969) 3728–3739.
[7] F.H. Stillinger, T.A. Weber, Packing structures and transitions in liquids and solids, Science 225 (1984) 983–989.
[8] T.A. Weber, F.H. Stillinger, The effect of density on the inherent structure in liquids, J. Chem. Phys. 80 (1984) 2742–2746.
[9] T. A Weber, F.H. Stillinger, Supercooled liquids, glass transitions, and the Kauzmann paradox, J. Chem. Phys. 88 (1988) 7818–7825.
[10] (a) J.D. Bryngelson, P.G. Wolynes, Spin glasses and the statistical mechanics of protein folding, Proc. Natl. Acad. Sci. USA 84 (1987) 7524–7528
(b) J.D. Bryngelson, P.G. Wolynes, Intermediates and barrier crossing in a random energy model (with applications to protein folding), J. Phys. Chem. 93 (1989) 6902–6915.
[11] C.A. Angell, Perspective on the glass transition, J. Phys. Chem. Sol. 49 (1988) 863–871.
[12] F.H. Stillinger, P.G. Debenedetti, Supercooled liquids and the glass transition, Nature 410 (2001) 259–267.
[13] E. La Nave, S. Mossa, F. Sciortino, Potential energy landscape equation of state, Phys. Rev. Lett. 88 (2002) 1–4, 225701.
[14] A. Scala, L. Angelani, R. Di Leonardo, G. Ruocco, F. Sciortino, A stroll in the energy landscape, Philos. Mag. Part B 82 (2002) 151–161.
[15] S. Mossa, C. Donati, E. La Nave, F. Sciortino, H.E. Stanley, P. Tartaglia, Dynamic and configurational entropy in the Lewis Wahnström Model for supercooled

orthoterpohenyl, Phys. Rev. Part E 65 (2002) 1–13, 041205.
[16] P.G. Debenedetti, F.H. Stillinger, T.M. Truskett, The equation of state of an energy landscape, J. Phys. Chem. Part B 103 (1999) 7390–7397.
[17] C.A. Angell, The glass transition, Pergammon Encyclopedia of Materials, Sci. Technol. 4 (2001) 3365, We note the recent evidence (see ref. [60] below), based on information available in ref [9], that the major part of the jump in heat capacity at T_g, when observed at constant pressure, is due to a jump in vibrational, not configurational, heat capacity.
[18] W. Kauzmann, The nature of the glassy state and the behavior of liquids at low temperatures, Chem. Rev. 43 (1948) 219–256.
[19] A.Q. Tool, Relation between inelastic deformability and thermal expansion of glass in its annealing range, J. Am. Ceram. Soc. 29 (1946) 240–253.
[20] V. Velikov, C.A. Angell, S. Borick, Molecular glasses with high fictive temperatures, J. Phys. Chem. 106 (2002) 1069–1080.
[21] Y-Z Yue, J. deC. Christiansen, S.L. Jensen, Determination of the fictive temperature for a hyperquenched glass, Chem. Phys. Lett. 357 (2002) 20–24.
[22] C.T. Moynihan, M.A. DeBolt, A.J. Easteal, J.C. Tucker, Dependence of the fictive temperature of glass on cooling rate, J. Am. Ceram. Soc. 59 (1976) 12–16.
[23] C.A. Angell, S. Borick, M. Grabow, Glass transitions and first order liquid–metal-to-semiconductor transitions in 4-5-6 covalent systems, J. Non-Cryst. Solids. 205–207 (1996) 463–471.
[24] S. Aasland, P.F. McMillan, Density-driven liquid–liquid phase separation in the system Al_2O_3–Y_2O_3, Nature 369 (1994) 633–636.
[25] M.C. Wilding, P.F. McMillan, A. Navrotsky, Thermodynamic and structural aspects of the polyamorphic transition in yttrium and other rare-earth aluminate liquids, Physica Part A 314 (2002) 379–390.
[26] H. Beck, H.-J. Gunterodt (Eds.), Glassy Metals II, Tracts in Applied Physics, 53, Springer, Heidelberg, Germany, 1983.
[27] J. Perel, B.E. Kalensher, J.F. Mahoney, R. Mehrabian, K.E. Vickers, Electrohydrodynamic generation of submicron particles for rapid solidification, Rapid Solidification Processes, Princeton Technol. (Proc. Intern. Conf. 1977), 1978, p. 258.
[28] V. Velikov, S. Borick, C.A. Angell, The glass transition of water, based on hyperquenching experiments, Science 294 (2001) 2335–2338.
[29] G.P. Johari, Does water need a new T_g?, J. Chem. Phys. 116 (2002) 8067–8073.
[30] Y-Z. Yue, C.A. Angell. Aging dynamics vs. crystallization in good and poor glassformers: 'shadow' glass transitions resolve the vitreous water T_g controversy, Nature (under review).
[31] L-M. Martinez, C.A. Angell, Chemical order lifetimes in liquids and a second fictive temperature for glassformers, Physica Part A: Stat. Mech. Appl. 314 (2002) 548–559.
[32] F.H. Stillinger, T.E. Weber, Chemical reactions in liquids: molecular dynamics simulation for sulfur, J. Chem. Phys. 85 (1986) 6460–6469.
[33] S.K. Kumar, J.F. Douglas, Gelation in physically associating polymer solutions, Phys. Rev. Lett. 87, (1987) art. no. 188301.
[34] J. Fan, C.A. Angell, Relaxational transitions and ergodicity breaking within the fluid state: the sugars fructose and galactose, Thermochimica Acta. 280 (1996) 523–530.
[35] W. Kauzmann, Some factors in the interpretation of protein denaturation, Adv. Protein Chem. 14 (1959) 1–63.
[36] A. Zipp, W. Kauzmann, Pressure denaturation of Metmyoglobin, Biochemistry-US 12 (1973) 4217–4228.
[37] I.D. Kuntz, W. Kauzmann, Adv. Protein Chem. 28 (1976) 239–343.
[38] W. Kauzmann, Thermodynamics of unfolding, Nature 325 (1987) 763–767.
[39] L-M. Wang, C.A. Angell, Electrospray technique for the study of liquid energetics by hyperquenched glass calorimetry, Phys. Rev. Part B, under review.
[40] L.M. Holzmann, T.F. Kelly, W.N.G. Hitchon, Crystal nucleation in submicron droplets of pure elements, Mat. Res. Soc. Symp. Proc. 321 (1994) 233–238.
[41] Y.W. Kim, H.M. Lin, T.F. Kelly, Amorphous solidification of pure metals in submicron spheres, Acta Metall. 37 (1989) 247–255.
[42] C.A. Summers, R.A. Flowers II, Protein renaturation by the liquid organic salt ethylammonium nitrate, Protein Sci. 9 (2000) 2001–2008.
[43] J.A. Garlitz, G.E.O. Borgstahl, R.A. Flowers II, C.A. Summers, Ethyl ammonium nitrate, a protein crystallization agent, Acta Crystalographia Part D: Biol. Cryst. Part D 55 (1999) 2037–2038.
[44] L.-M. Wang, C.A. Angell, V. Velikov, Direct determination of kinetic fragility indices of glassforming liquids by differential scanning calorimetry: Kinetic vs. thermodynamic fragilities, J. Chem Phys. 117 (2002) 10184–10192.
[45] R. Böhmer, C.A. Angell, Correlations of the nonexponentiality and state dependence of mechanical relaxations with bond connectivity in Ge–As–Se supercooled liquids, Phys. Rev. Part B. 45 (1992) 10091–10094.
[46] R. Böhmer, C.A. Angell, K.L. Ngai, D.J. Plazek, Nonexponential relaxations in strong and fragile glassformers, J. Chem. Phys. 99 (1993) 4201–4209.
[47] D.J. Plazek, K.L. Ngai, Correlation of polymer segmental chain dynamics with temperature-dependent timescale shifts, Macromology 24 (1991) 1222–1224.
[48] C.A. Angell, D.L. Smith, Test of the entropy basis of the VTF equation: dielectric relaxation of polyalcohols near T_g, J. Phys. Chem. 86 (1982) 3845–3852.

[49] E. Mayer, New method for vitrifying water and other liquids by rapid cooling of their aerosols', J. Appl. Phys. 58 (1985) 663–667.
[50] E. Mayer, Vitrification of pure liquid water, J. Microsc. 140 (1985) 3–15.
[51] G.P. Johari, A. Hallbrucker, E. Mayer, Thermal Behavior of several hyperquenched organic glasses, J. Phys. Chem. 93 (1989) 2648–2652.
[52] N.O. Birge, Specific-heat spectroscopy of glycerol and propylene glycol near the glass transition, Phys. Rev. Part B 34 (1986) 1631–1642.
[53] J.C. Dyre, Energy master equation: a low-temperature approximation to Bassler's random-walk model, Phys. Rev. Part B 51 (1995) 12276–12294.
[54] C.A. Angell, Dynamic processes in ionic glasses, Chem. Rev. 90 (1990) 523–542.
[55] A. Matagne, M. Jamin, E.W. Chung, C.V. Robinson, S.E. Radford, M.C. Dobson, Thermal unfolding of an intermediate is associated with non-Arrhenius kinetics in the folding of hen lysozyme, J. Mol. Biol 297 (2000) 193–210, and references therein.
[56] S. Cinelli, G. Onori, A. Santucci, Effect of aqueous alcohol solutions on the thermal transition of lysozyme: a calorimetric study, J. Phys. Chem. Part B 101 (1997) 8029–8034.
[57] M. Hirai, S. Arai, H. I wase, T. Takizawa, Small-angle X-ray scattering and calorimetric studies of thermal conformational change of lysozyme depending on pH, J. Phys. Chem. Part B 102 (1998) 1308–1313.
[58] S.E. Radfold, C.M. Dobson, P.A. Evans, The folding of hen lysozyme involves partially structured intermediates and multiple pathways, Nature 358 (1992) 302–307.
[59] M.R. Eftink, R. Ionescu, Thermodynamics of protein unfolding: questions pertinent to testing the validity of the two-state model, Biophys. Chem. 64 (1997) 175–197, and references therein.
[60] Y.Z. Yue, J. de, C. Christiansen, S.L. Jensen, Physical aging in a hyperquenched glass, Appl. Phys. Lett. 81 (2002) 2983–2985.
[61] C.A. Angell, Y.Z. Yue, L-M. Wang, J.R.D. Copley, S. Borick, S. Mossa, Potential energy, relaxation, vibrational dynamics and the boson peak, of hyperquenched glasses', J. Phys. Condensed Matt. 15 (2003) 51051–51058.
[62] P.G. Wolynes, J.N. Onuchic, D. Thirumalai, Navigating the folding routes, Science 267 (1995) 1619–1620.
[63] J.D. Bryngelson, J.N. Onuchic, N.D. Socci, P.G. Wolynes, Funnels, pathways, and the energy landscape of protein folding: a synthesis, Proteins: Struct. Funct. Gen. 21 (1995) 167–195.
[64] C.L. Brooks, M. Gruebele, J.N. Onuchic, Chemical physics of protein folding, Proc. Natl. Acad. Sci. USA 95 (1998) 11037–11038.
[65] E. Shakhnovich, V. Abkevich, O. Ptitsyn, Conserved residues and the mechanism of protein folding, Nature 379 (1996) 96–98.
[66] L. Mirny, E. Shakhnovich, Evolutionary conservation of the folding nucleus, J. Mole. Bio. 308 (2001) 123–129.
[67] J.N. Onuchic, Z. LutheySchulten, P.G. Wolynes, Theory of protein folding: The energy landscape perspective, Annu. Rev. Phys. Chem. 48 (1997) 545–600.
[68] E. Shakhnovich, A.R. Fersht, Folding and binding–overview, Curr. Opinion Struct. Biol. 8 (1998) 65–67.
[69] C.A. Tulk, C.J. Benmore, P.A. Egelstaff, D.D. Klug, J. Neuefeind, B. Tomberli, J. Urquidi, Structural studies of several distinct metastable forms of amorphous ice, Science 297 (2002) 1320–1324.